Optical Homogeneity of Gyroscope Blanks for the Gravity Probe-B Experiment

J. M. De Freitas and M. A. Player
Engineering Physics Group, Department of Engineering,
University of Aberdeen, Aberdeen AB9 2UE. UK.

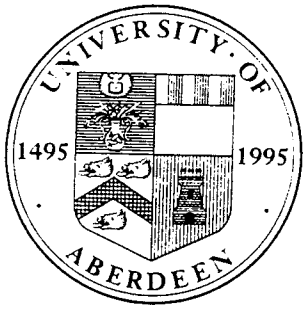

Presented at the Applied Optics and Opto-electronic Conference,
5-8 Sept. 1994, University of York, UK.
This work has been supported by a grant from Stanford University.

Abstract

The Gravity Probe-B is a relativity gyroscope experiment being developed by NASA and Stanford University to test the prediction of the general theory of relativity by observing the extent of precession of the gyroscope in orbit around the Earth. The rotor of the proposed gyroscope will be made of vitreous silica. This paper describes the measurement of the optical homogeneity (or mass density distribution) of fused quartz cubes of side 50mm. The variations in refractive index Δn, across the faces of the cubes are measured with a unique scanning interferometer, and are of the order of $\Delta n = 3 \times 10^{-6}$ with a precision better than 10^{-7}, achieved through orthogonal polynomial fitting of the optical path difference surfaces. First and second order moments of the density variations are calculated from three orthogonal projections.

Background

The Gravity Probe-B (GP-B) is a relativity gyroscope (gyro) experiment being developed by the US National Aeronautics and Space Administration (NASA) and Stanford University, to test the predictions of the general theory of relativity by observing the extent of precession of gyroscopes in polar orbit around the Earth. The experiment will carry out high precision measurements of two general relativistic effects. The larger *geodetic effect* is the precession of a gyroscope due to the curvature of space produced by the mass of the Earth. The smaller *motional effect*, predicted by Lense and Thirring [1], induces precession in a gyroscope due to the frame dragging caused by the rotation of the Earth. At a 650km polar orbit, the geodetic effect is 6.6 arc sec/year, and the motional effect is 42 milli-arc sec/year [2].

The probe itself consists of four gyroscopes, a telescope for reference star tracking and a proof-mass arrangement for enhanced drag-free performance - all being held at liquid Helium temperature. The precessions of the assembly of the gyros will be measured with reference to the fixed star Rigel. Two gyros will rotate clockwise while the other two (as experimental controls) will be anticlockwise. The gyros are suspended via servo-controlled electrostatic bearings, and readout is by detection of the London magnetic moment of the superconducting niobium coated gyroscopes [2].

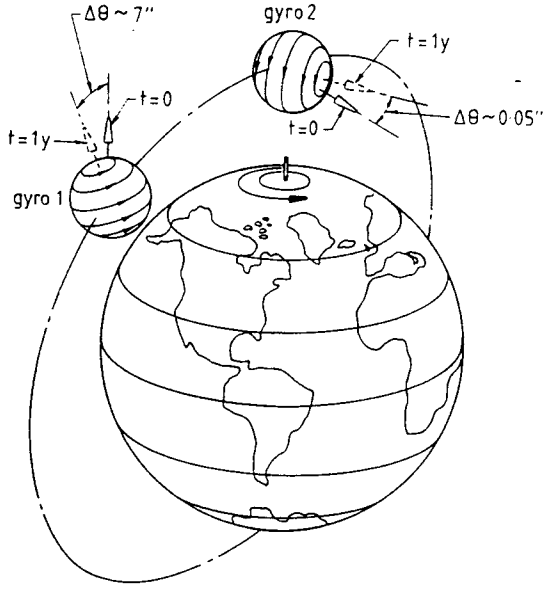

Figure 1: Motional and geodetic effects on gyros.

The aim of the GP-B experiment is to achieve a precision of 1 part in 10^4 for the geodetic effect, and 1% for the motional effect, by measuring the precessions to a precision of about 1 milli-arc sec/year. The consequent requirement on torques arising from mass imbalance due to inhomogeneity of the gyroscope rotor material in terms of mass density ρ, is

$$\frac{\Delta\rho}{\rho} \leq 3 \times 10^{-7}, \tag{1}$$

if residual accelerations in the 'drag-free' reference frame are to be less than $10^{-9}g$, where g is the acceleration due to gravity. The major torques arise from rotor dipole moment interacting with the residual gravitational field, and from the quadrupole moment interacting with the field gradient. The corresponding requirement on the incremental mass dipole moment ΔD is,

$$\Delta D \leq 2.5 \times 10^{-8} a^4, \tag{2}$$

where a is the cube side. The shift in the centroid resulting from the mass imbalance, must therfore satisfy,

$$\Delta\overline{x} \leq 2.5 \times 10^{-8} a. \tag{3}$$

These requirements have significant consequences for the choice, manufacture and screening of the material. The material chosen for rotor manufacture was vitreous silica. This has two advantages: (i) with careful preparation of vitreous silica high optical homogeneity is possible, and (ii) the optical homogeneity can be measured by classical optical techniques such as interferometry. The technique developed for measurement of optical homogeneity is to move the sample (in the form of 50mm cube) within an index-matching immersion tank across the beam of one arm of a high precision interferometer, and observe the change in optical pathlength. For our 50mm sized fused silica samples of refractive index 1.457, the total change in mass dipole moment ΔD, must not exceed 3.44×10^{-5} gcm, or equivalently, $\Delta\overline{x} \leq$ 1.25nm. This is equivalent to a point mass of 34μg or less at a distance of 1cm from the centre of gravity of the sample! The challenging aspect of this work is to detect such small mass imbalances with high sensitivity. The aim of this presentation therefore, is to give the current status of development of the homogeneity instrumentation and typical results from a small batch of gyroscope blanks.

Moment Expansion of Refractive Index

The refractive index n is a function of position i.e. $n = n(x, y, z)$ provided temperature and pressure remain constant. This may be rewritten as $n = \overline{n} + \Delta n$, as Δn is indirectly measured by the interferometer; $\overline{n}$ is the mean refractive index through the cube sample. Consider the Fourier expansion of Δn,

$$\Delta F(k_x, k_y, k_z) = \int\int\int \Delta n(x, y, z) e^{-j(k_x x + k_y y + k_z z)} dx dy dz,$$

which is conveniently rewritten vectorially as,

$$\begin{aligned} \Delta F(\mathbf{k}) &= \int \Delta n(\mathbf{r}) e^{-j(\mathbf{k}.\mathbf{r})} dv \\ &= \int \Delta n(\mathbf{r}) dv - j \int (\mathbf{k}.\mathbf{r}) \Delta n(\mathbf{r}) dv - \int (\mathbf{k}.\mathbf{r})^2 \Delta n(\mathbf{r}) dv \\ &\quad + \ldots + (-j)^m \int (\mathbf{k}.\mathbf{r})^m \Delta n(\mathbf{r}) dv + \ldots \end{aligned} \tag{4}$$

Moreover, $\int (\mathbf{k}.\mathbf{r})^m \Delta n(\mathbf{r}) dv$ relates to the mth moment of refractive index change. The average mth power displacement of the centroid associated with the change in moment of order m, is given by

$$\Delta \overline{(\mathbf{k}.\mathbf{r})^m} = \frac{\int (\mathbf{k}.\mathbf{r})^m \Delta n(\mathbf{r}) dv}{\int n(\mathbf{r}) dv}. \tag{5}$$

Equating coefficients of components of $\mathbf{k}$ on both sides of equation (5) we have

$$\Delta \overline{x^p y^q z^r} = \frac{\int\int\int x^p y^q z^r \Delta n(x, y, z) dx dy dz}{\int\int\int n(x, y, z) dx dy dz} \tag{6}$$

with $(p, q, r = 0, 1, \ldots; p + q + r = m)$. Equation (6) can be expressed in terms of the optical path length variation $\Delta P(u, v)$ $(u, v = x, y, z; u \neq v)$ obtained from the interferometer, provided that either p,q or r is zero. Moreover, the dipole and quadrupole moments obtained from expansion of the refractive index are identical to the dipole and quadrupole moments obtained from the expansion of the measured optical path length. However, for higher orders (i.e. $m > 2$) the moments from optical path length expansion differ from those obtained from refractive index expansion.

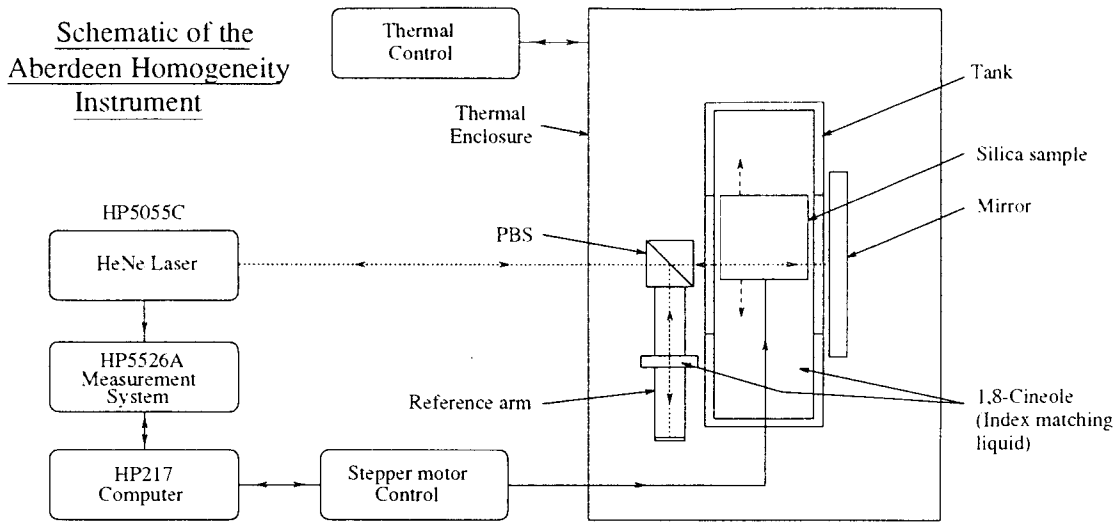

Figure 2: Experimental setup.

The homogeneity instrument

The homogeneity instrument is a dedicated computerised narrow beam scanning heterodyne interferometer. It is built around the Hewlett-Packard 5526A laser measurement system, and incorporates an HP 217 computer for data acquisition and scanning preocedures. A schematic of the instrument is shown in Figure (2).

The resolution of the HP 5526A laser measurement system is $\lambda/1440$ (0.44nm) when in combination with the $\times 36$ resolution extender (HP10579-60004), however we have in the past noticed a noise jitter, thereby reducing the workable resolution to about 2.2nm [3, 4]. This resolution could be substantially reduced to about 0.2nm by using a simple analog phase meter [5]. The system, from a resolution perspective, is capable of detecting optical path difference features within a 5nm range.

The thermal coefficient of refractive index (dn/dT) for fused silica is 1.04×10^{-5}/K, and as such it is necessary to control the environment to within a few milli-°C. This has been achieved by building an active servo-controlled thermal enclosure around the interferometer [4]. Moreover, the reference arm has been carefully designed to compensate for thermal drifts in the measurement arm [5].

The surface features of the sample are removed by immersing it in 1,8-cineole,

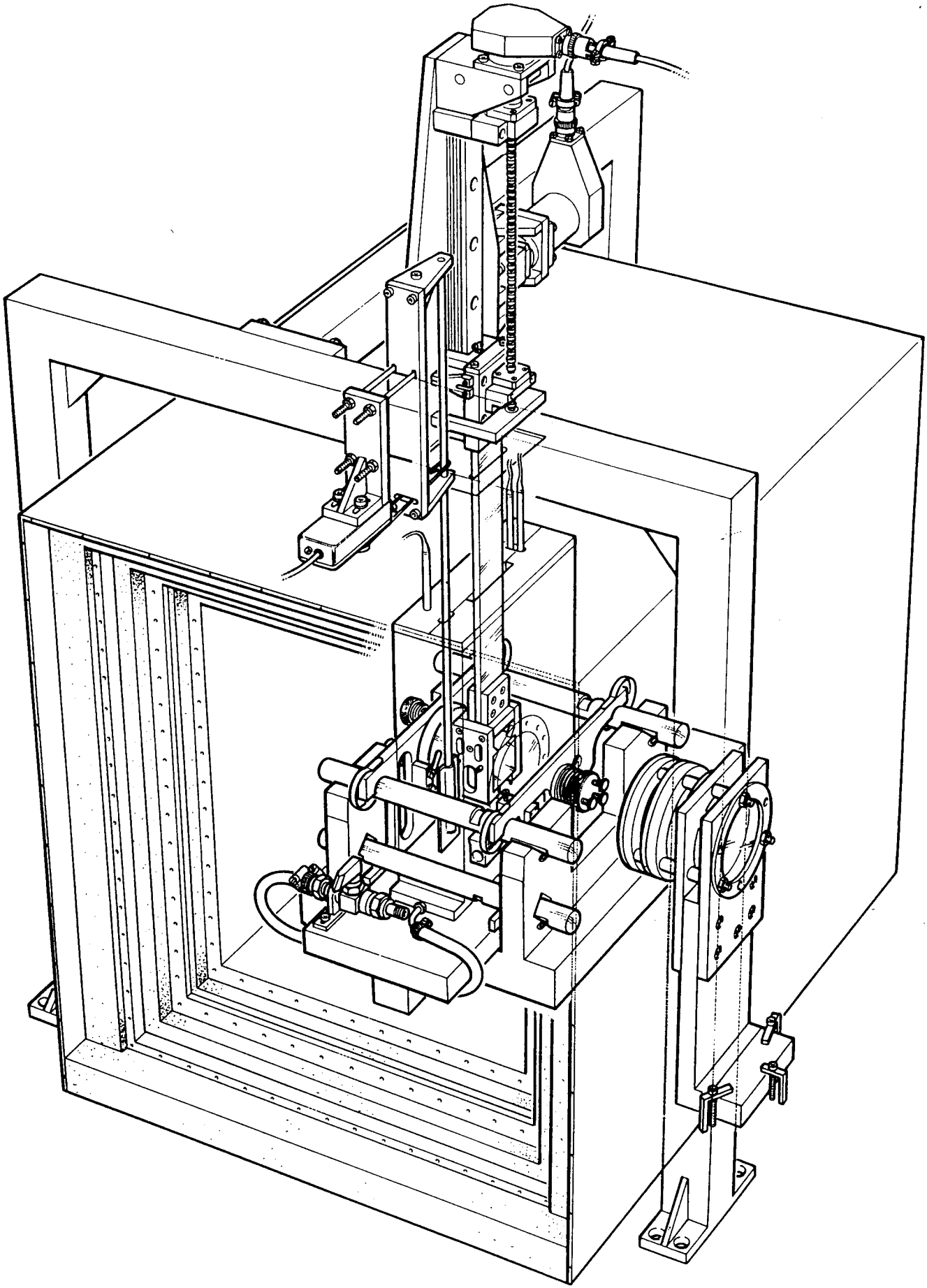

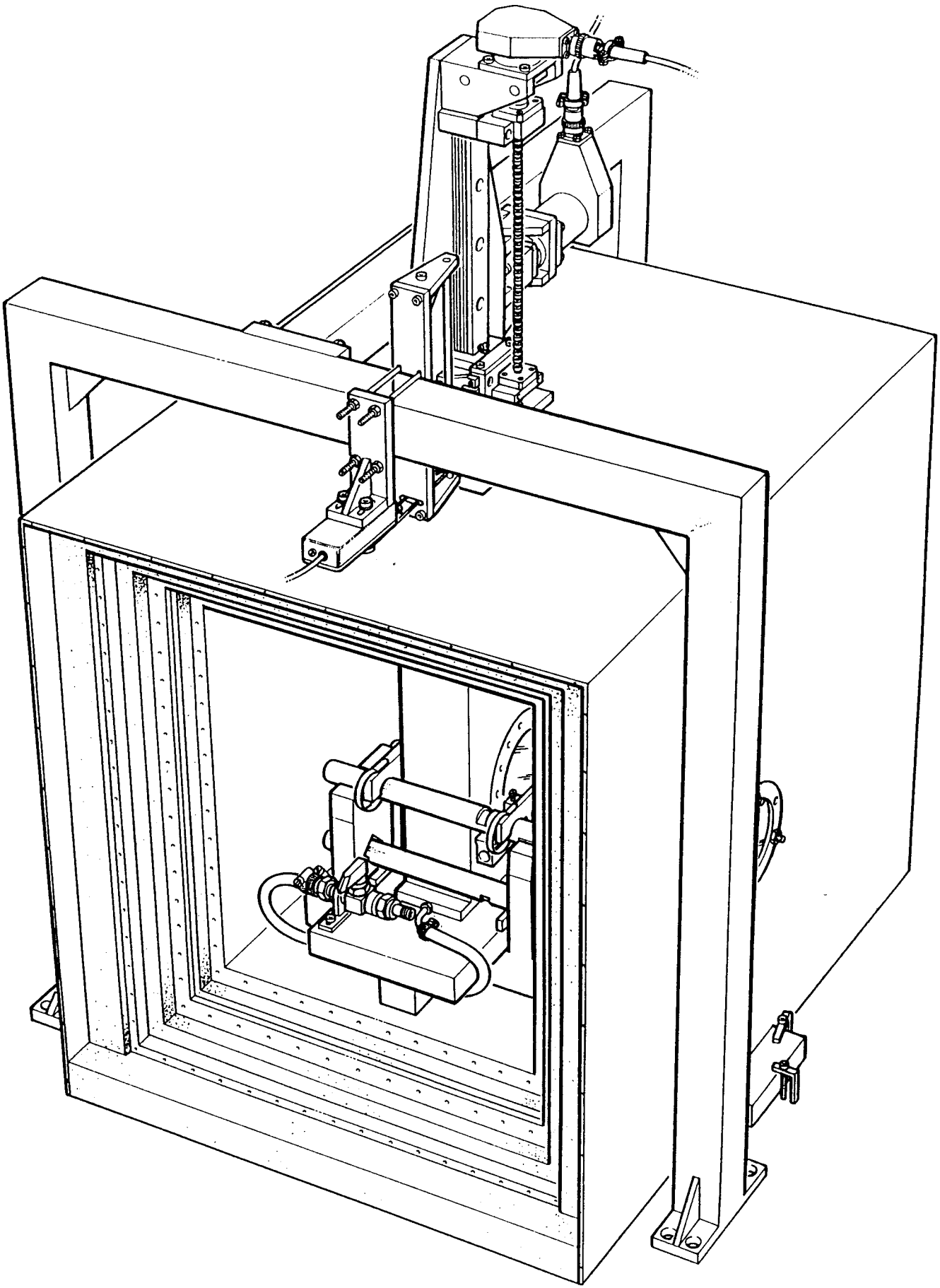

which matches vitreous silica in refractive index at about 17.49°C. Refractive index mismatching allows the effects of non-parallel faces to influence the the sensitivity of the measurements. For a worst case condition of 6 arcmin parallelism error, and a worst case mismatch of refractive index between the cineole and the sample of $\delta n \sim 10^{-5}$, an additional shift in the centroid position of approximately 0.06nm will result. It is therefore necessary to immerse the sample in the index matching liquid for periods up to a few days to ensure thermal equilibrium, and to mantain the temperature at 17.49°C to within a few m°C, before and during an experiment. Further details on design and fabrication of the homogeneity instrument can obtained from [4].

Experimental results and analysis

In the experiments reported here, measurements were taken along vertical lines over the surface of the sample as this scanning mode is least susceptible to noises coupled from the translator system. The samples were obtained from Heraeus Quarzschmelze GmbH, Germany.

Figure 3 shows the convention adopted for viewing and scanning. The datum point is denoted by a small '+' drawn at the top left hand corner on one of the surfaces of the sample - which we call the 'reference' or 'first' surface. The two other orthogonal surfaces are the 'second' and 'third' surfaces respectively; they also have datum positions marked with circles. The datum position is at (0,0) in all the scans reported. With the coordinate system as shown we can associate the reference, second and third surface OPD scan results with ΔP_x, ΔP_y and ΔP_z respectively. For each surface, when the datum position is at the top left hand corner, the scan motion is always vertical.

The experimental conditions are given in Table 1. Figures (4) and (5) show the experimental scan results of the reference surface of sample 93H79. The peak-to-peak change in refractive index of 3×10^{-6} is seen to be more than ten times larger than the worst case requirement for the GP-B gyroscope rotor. However, the repeatability between scans has been good in well run experiments for samples with relatively large refractive index variations. For example, the difference between SURF37 and SURF38, shown in Figure (6), has a peak-to-peak difference of 9.8nm, with instrument noise contributing largely to this difference. When the two surfaces

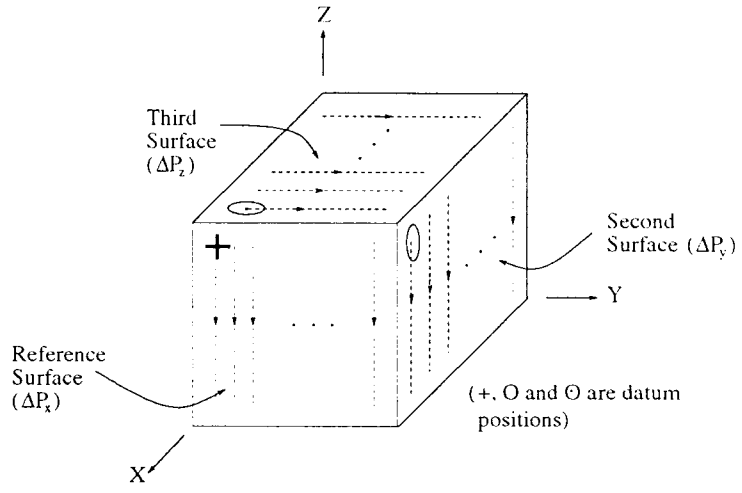

Figure 3: Scanning and viewing convention. Broken lines show the action of the scanning procedure for the three surfaces relative to each other.

are least squares fitted (see below) this difference is reduced to 5.1nm.

A least squares orthogonal polynomial fitting procedure [6] was used to smooth the data, to provide a comparison with the Zernike polynomials obtained from broad beam methods provided by the manufacturer, and for archival purposes. Fifty terms (9th order polynomials) were found to be satisfactory for the scans reported. Figures (7)-(9) show the three orthogonal OPD surfaces and their residuals (i.e. the difference between the data and the fit). The residuals are plotted by placing the line scans head-to-tail. In all the fitted surfaces shown, the peak-to-peak residuals are within a range of 5nm, and as such the fitting procedure gives us a sensitivity better than $\Delta n = 10^{-7}$ over 50mm. Note too, that the spectral distribution of the residuals is similar to

Dataset	View	T	ΔT	P	ΔP	OPD_{p-p}	Polar.	Δn
		(°C)	(m°C)	(mbar)	(mbar)	(nm)	state	$\times 10^{-6}$
SURF37	ΔP_x	17.477	+2	1020.1	+2.5	139	↑	3.0
SURF38	ΔP_x	17.484	+1	1025.1	+1.8	142	↑	3.1
SURF63	ΔP_y	17.396	+2	1010.9	−0.4	117	↑	2.5
SURF68	ΔP_z	17.490	–	–	–	109	↑	2.4

Table 1: Experimental details of sample 93H79.

Dataset	View	Dipole (10^{-5} g.cm)			Centroid shift (nm)		
		ΔD_x	ΔD_y	ΔD_z	$\Delta\overline{x}$	$\Delta\overline{y}$	$\Delta\overline{z}$
SURF38	ΔP_x	–	8	21	–	5	12
SURF63	ΔP_y	8	–	19	5	–	13
SURF68	ΔP_z	8	13	–	5	8	–

Table 2: Components of the dipole moment of sample 93H79.

a Gaussian white noise distribution. Prior to the modification of the reference arm, which now balances the interferometer, a quasi-periodic noise distribution was observed [5]. It is suggetsed here that the quasi-periodic behaviour of the noise was due to the small drifts in laser frequency in our original interferometer set-up, as OPD errors are directly proportional to drifts in frequency. The residuals offer a good picture of the system noise during scanning, but there is no simple way of assessing system drifts due to changes in temperature, pressure, temporal variations in refractive index along the cineole liquid path, and the effect of cineole vapour concentration changes (or its partial vapour pressures).

Table 2 shows the results of the calculation of the dipole moments from the three orthogonal planar projections. Clearly, this sample does not meet the requirements. The average of the total centroid shift is 15 ± 1nm, where we have estimated the root mean square (rms) values for the shift in the centroid position and the dipole moment, by averaging the eight possible combinations of the $x-$, $y-$ and $z-$directions in the table. The corresponding rms error for the dipole moment is $\pm 1 \times 10^{-5}$gcm.

Table 3 contains the incremental components of the quadrupole moment and second order centroid shifts for the sample 93H79.

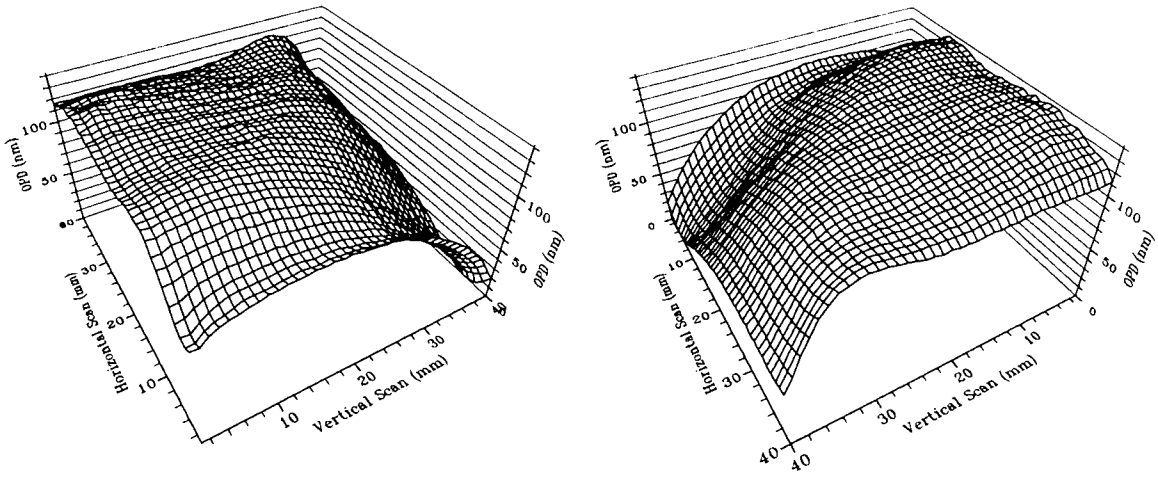

(a) (b)

Figure 4: Two dimensional OPD: First surface. (a) Front (b) back view of SURF38.

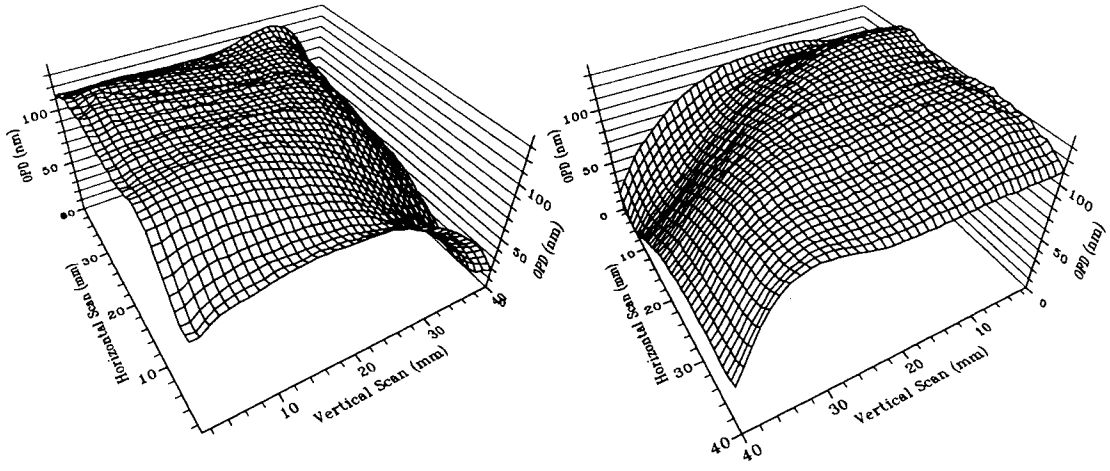

(a) (b)

Figure 5: Two dimensional OPD: First surface. (a) Front (b) back view of SURF37.

Dataset	Quadrupole Moment (10^{-5} g.cm^2)					
	ΔQ_{xx}	ΔQ_{yy}	ΔQ_{zz}	ΔQ_{xy}	ΔQ_{xz}	ΔQ_{yz}
SURF38	–	−5	−12	–	–	−7
($\Delta\overline{uv}$ /μm^2)	–	(31)	(74)	–	–	(43)
SURF63	5	–	−8	–	−2	–
($\Delta\overline{uv}$ /μm^2)	(31)	–	(49)	–	(12)	–
SURF68	4	−5	–	−0.4	–	–
($\Delta\overline{uv}$ /μm^2)	(25)	(31)	–	(2.5)	–	–

Table 3: Components of the quadrupole moment of sample 93H79. The uv of $\Delta\overline{uv}$ are identical to the subscripts of Q in each column.

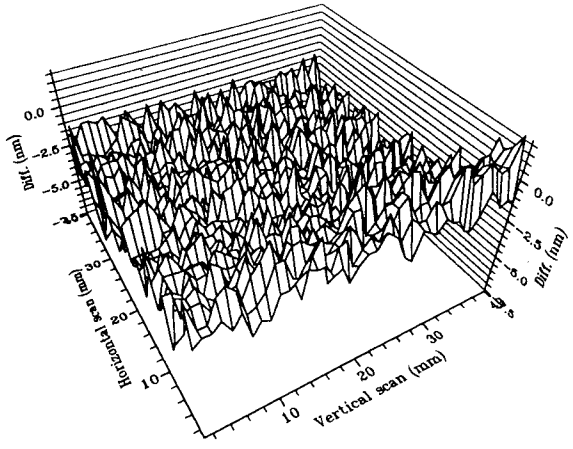

Figure 6: Difference between SURF37 and SURF38.

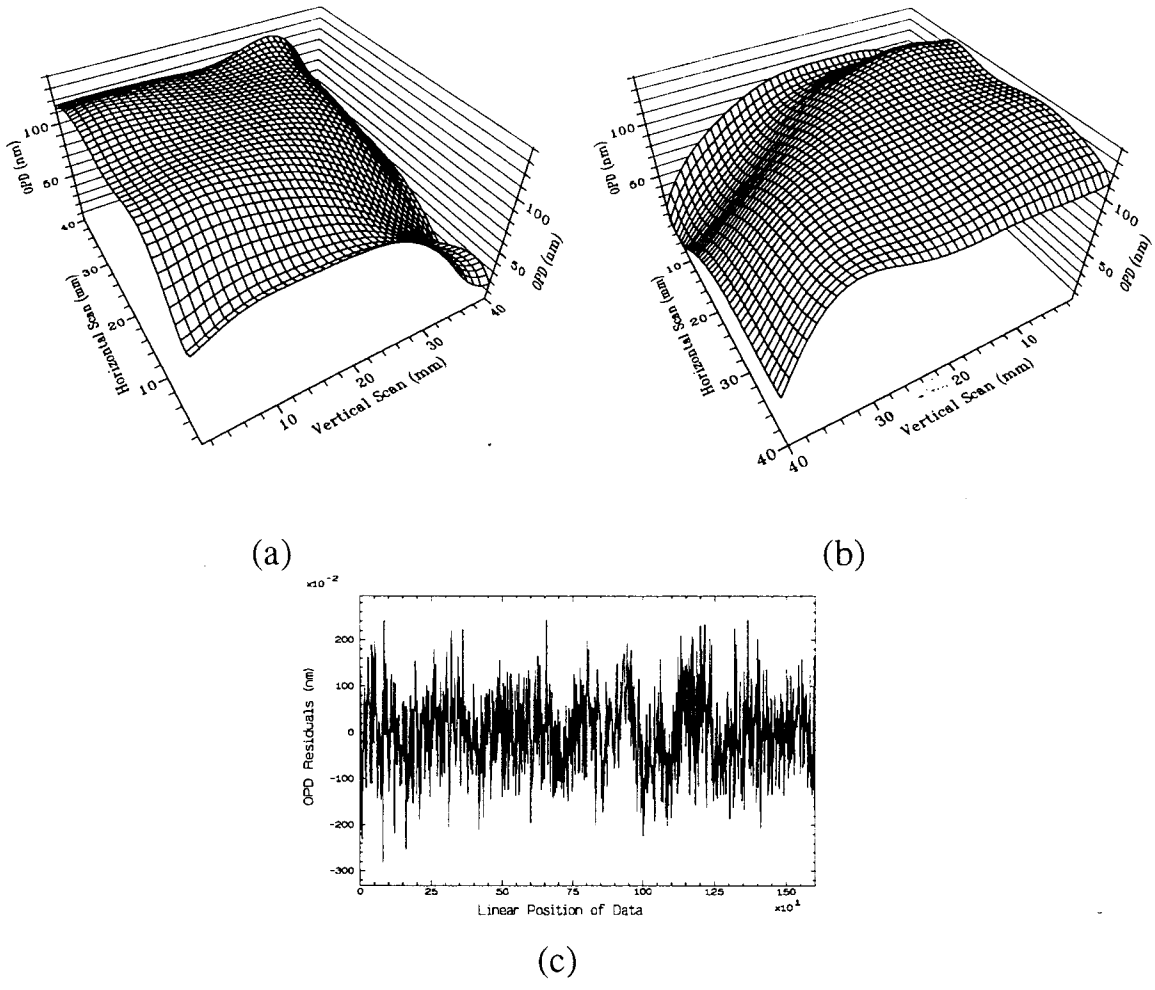

Figure 7: Least squares polynomial fit to first surface data (SURF38). (a) Front (b) Back view. (c) Residuals of polynomial fitting.

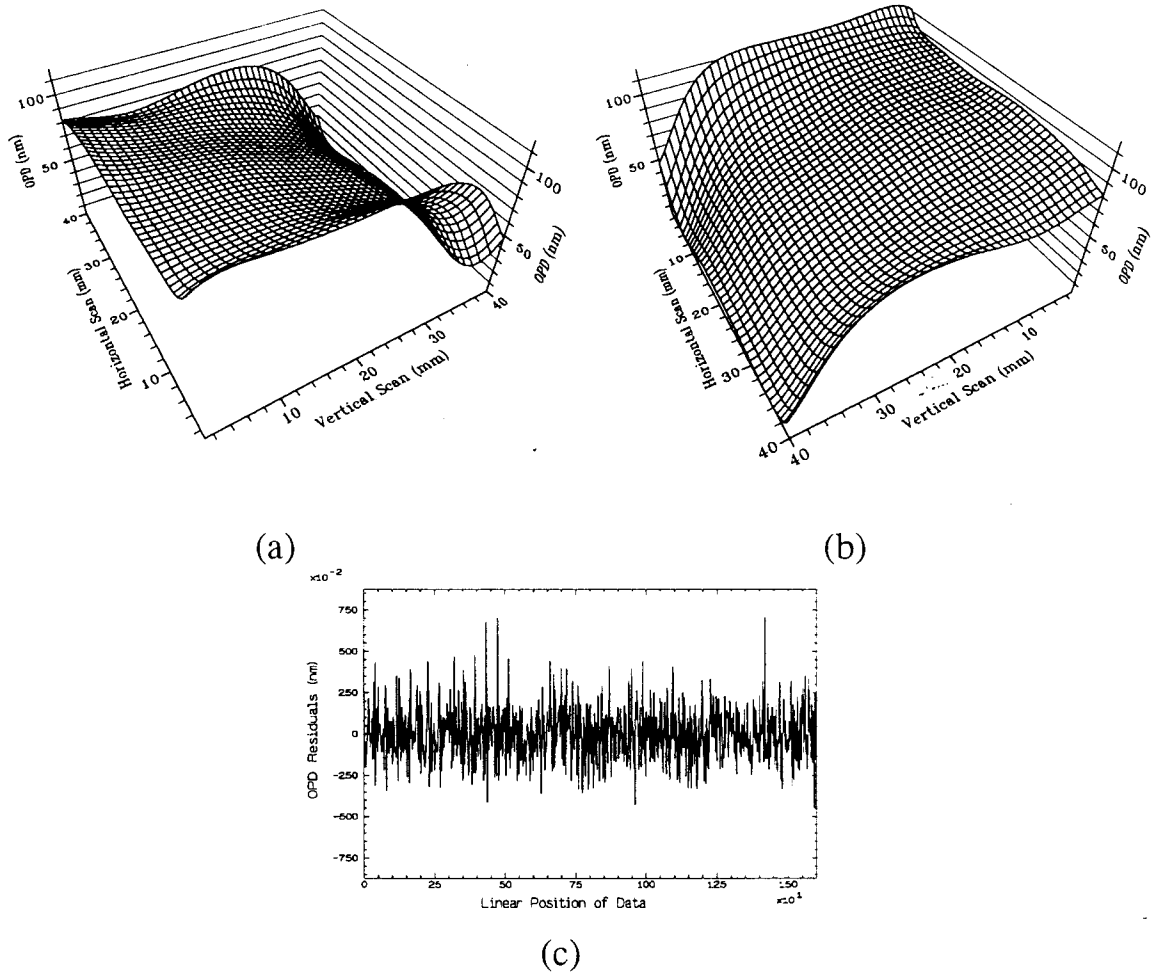

Figure 8: Least squares polynomial fit to second surface data (SURF63). (a) Front (b) Back view. (c) Residuals of polynomial fitting.

Concluding Remarks

The manufacture of the GP-B gyroscope rotor includes two important features: (a) the production of a very homogeneous material in terms of mass density; (b) the measurement of the homogeneity to an exceedingly high precision; for vitreous silica, the measurement requires a precision in refractive index of a few parts in 10^8. We have demonstrated that we could measure the refractive index variation to a precision better than one part in 10^7, with excellent repeatability of features to within 5nm optical path difference, in moderately large refractive index changes. The measurement system appears to be limited by the noise associated with temporal variations in refractive index of the index matching liquid in the measurement arm during scanning. However, there are significant advantages over homogeneity instruments which use differential heterodyne interferometry, (e.g. [7]), and most forms of broad beam interferometry [4]. The primary advantage of our scanning system is that it measures directly the variations of refractive index. This is in contrast to the indirect integration method of [7] and reconstruction of wavefronts, though it is believed that there are future prospects for phase shifting interferometry in this area. All indirect methods depend on the accuracy and noise filtering properties of suitable algorithms.

Further work includes the use of 2D spectral analysis of the three orthogonal projections, which in principle only provides estimates of dipole and quadrupole moments, but with the additional possibility of detecting a refractive index spectral signature for vitreous silica. There is also some interest in limited view reconstruction of the 3D distribution of refractive index.

References

[1] C. M. Will. *Theory and Experiment in Gravitational Physics.* Cambridge Univ. Press, 1981.

[2] J. M. Lockhart, W. S. Cheung, and D. K. Gill. Superconducting Thin-Film Gyroscope Readout for Gravity Probe-B. *IEEE Trans. Instr. Meas.*, IM-36:170–174, 1987.

[3] M. A. Player. Interim Report on Quartz Homogeneity Measurements. Technical report, Aberdeen University., 1985.

[4] G. Edgar. *A Precision Interferometric Optical Heterogeneity Mapping System.* PhD thesis, University of Aberdeen, Aberdeen. UK, 1990.

[5] J. M. De Freitas. *Interferometric Characterisation of Refractive Index Variations in Vitreous Silica.* PhD thesis, University of Aberdeen, Aberdeen. UK, 1994.

[6] I. K. Crain and B. K. Bhattycharyya. Treatment of Non-equispaced Two-dimensional Data With a Digital Computer. *Geoexploration*, 5:173–194, 1967.

[7] N. Bobroff, A. E. Rosenbluth, and M. Hatzakis. Scanning Differential Interferometer to Measure Index Heterogeneity. *Appl. Opt.*, 31:6622–6631, 1992.